IEEE Access
Multidisciplinary | Rapid Review | Open Access Journal

Received December 23, 2021, accepted January 19, 2022, date of publication January 26, 2022, date of current version February 4, 2022.

Digital Object Identifier 10.1109/ACCESS.2022.3146414

Switchable Multi-Wavelength Thulium-Doped Fiber Laser Using a Cascaded or Two-Segment Sagnac Loop Filter

TING LI[1], FENGPING YAN[1], DAN CHENG[1], QI QIN[1], YING GUO[1], TING FENG[2,3], ZHUOYA BAI[1], XUEMEI DU[1], YUPING SUO[4], AND HONG ZHOU[5]

[1]School of Electronic and Information Engineering, Beijing Jiaotong University, Beijing 100044, China
[2]Photonics Information Innovation Center, College of Physics Science and Technology, Hebei University, Baoding 071002, China
[3]Hebei Provincial Center for Optical Sensing Innovations, College of Physics Science and Technology, Hebei University, Baoding 071002, China
[4]Shanxi Provincial People's Hospital, Shanxi Medical University, Taiyuan 030012, China
[5]Department of Electronics, Information and Communication Engineering, Osaka Institute of Technology, Osaka 535-8585, Japan

Corresponding authors: Fengping Yan (fpyan@bjtu.edu.cn) and Ting Feng (wlxyft@hbu.edu.cn)

This work was supported by the National Natural Science Foundation of China (NSFC) under Grant 61827818, Grant 61620106014, and Grant 61975049.

ABSTRACT A switchable multi-wavelength thulium-doped fiber laser (TDFL) using either two-stage cascaded or two-segment Sagnac loop filters are proposed and analyzed. Both filters incorporate a 3-m and 1.7-m long polarization-maintaining fiber, which acts as a comb filter. By adjusting two polarization controllers, when the TDFL used a cascaded Sagnac loop filter, eight stable single-wavelength operations were obtained with easy switching among them. The wavelength range was 16.36 nm during the single-wavelength switchable operation, with the optical signal-to-noise ratio up to 55 dB. This TDFL can achieve at most quintuple-wavelength operation. When the TDFL used a two-segment Sagnac loop filter, we achieved single-wavelength and dual-wavelength switchable. This TDFL can achieve at most stable quadruple-wavelength operation. In dual-wavelength switchable operation, the maximum and minimum wavelength spacings were 21.78 nm and 1.50 nm. Due to its abundant range of wavelengths, the proposed TDFLs has great potential in wavelength-division multiplexing.

INDEX TERMS Multi-wavelength thulium-doped fiber laser, wavelength switchable, cascaded Sagnac loop filter, two-segment Sagnac loop filter.

I. INTRODUCTION

Multi-wavelength fiber lasers (MWFL) are attracting increased research attention because of their simple structure, good heat dissipation, portability, and high efficiency [1]–[3]. Because of their potential to broaden the channel capacity of communication systems, the development of multi-wavelength lasers near the 2-μm waveband has attracted particular research attention [4]–[6]. Using thulium-doped fiber as a gain medium, a laser can be excited in the 2-μm band with a higher self-focusing threshold and lower nonlinear effect than in the near-infrared band [7], [8]. Such a laser poses little risk to the eyes and finds applications in various fields, including laser radar, laser communication, and environmental remote sensing [9]–[11]. As one of the ideal signal sources in a wavelength-division multiplexing (WDM) system, the flexible wavelength switching of thulium-doped fiber lasers (TDFL) is an important indicator, and various structures of comb filters are widely utilized [12]–[14].

The common tunable devices in switchable TDFLs include the fiber Bragg grating (FBG), the fiber interferometer, the micro-electro-mechanical system, and silicon-based liquid crystals [15]–[18]. Feng *et al.* designed a stable and switchable four-wavelength erbium-doped fiber laser (EDFL) using a superimposed high-birefringence FBG [19]. This EDFL can be switched among fifteen lasing states: four single-wavelength states, six dual-wavelength states, four three-wavelength states, and one four-wavelength state, all with high stability. Jin *et al.* proposed a switchable dual-wavelength EDFL utilizing a few-mode FBG [20]. To increase the number of output wavelengths, Ying Guo *et al.* achieved a 60-wavelength laser

The associate editor coordinating the review of this manuscript and approving it for publication was Zinan Wang.

output within a 3 dB bandwidth in the 2-μm-band with a nonlinear dual-pass Mach-Zehnder interferometer filter [21]. Al-Alimi *et al.* introduced a wide bandwidth and a flat multi-wavelength Brillouin-erbium fiber laser based on dispersion-compensating fiber (DCF) and highly nonlinear optical fiber (HNLF) [22]. Its output can be up to 200 lasing wavelengths with an optical signal-to-noise ratio (OSNR) exceeding 15 dB and a flatness of 4.65 dB. In addition, there are several external items of equipment such as stress racks and taper machines that can improve the OSNR and the number of output wavelengths [15], [23], [24].

In this paper, we report on the design and demonstration of wavelength-switchable multi-wavelength TDFLs assisted by a cascaded Sagnac loop filter or a two-segment Sagnac loop filter. The transmission performances of two filters with different cascaded mode are analyzed theoretically and studied experimentally. When the filter is a cascaded Sagnac loop, the maximum number of output wavelengths without extra wavelength competition structure is five and a single-wavelength selection operation from 1986.35 to 2002.71 nm can be realized. When using a two-segment Sagnac loop as a comb filter, the maximum number of output wavelengths is reduced to four but the flexibility of wavelength selection is greatly improved. The influences of the two structures on laser stability and output power are compared in the following sections.

II. PRINCIPLE OF CASCADED FILTERS

A. CASCADED SAGNAC LOOP FILTERS

Fig. 1 shows the structure of cascaded Sagnac loop filters. High-birefringence (HiBi) polarization-maintaining fiber (PMF) Sagnac filter is a kind of all-fiber multi-wavelength comb filter with simple structure and easy fabrication, it is consisted by a PMF, a 3 dB optical coupler (OC) and a polarization controller (PC). The cascaded Sagnac loop filter contains two Sagnac filter and an isolator (ISO). The ISO ensures the unidirectional oscillation.

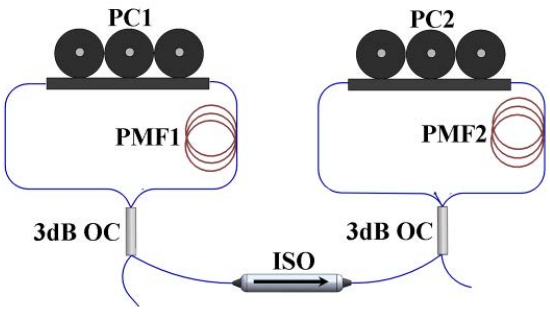

FIGURE 1. The structure of a cascaded Sagnac filter.

The transmission and the free spectral range (FSR) of individual Sagnac loop filter is [25]:

$$T = \sin^2\theta\cos^2(\frac{\pi L\Delta n}{\lambda})$$

$$\Delta\lambda = \frac{\lambda^2}{\Delta nL} \tag{1}$$

where θ is the rotation angle of polarized light. L is the length of PMF, Δn is the high-birefringence coefficient and λ is the central wavelength of the incident light. For the cascaded Sagnac filter, the transmitted light of the former filter provides the incident light for the latter. An isolator is sandwiched between the two filters to ensure unidirectional oscillation. The final transmittance after the cascade can be written as:

$$T_{cascaded} = T_1T_2 \tag{2}$$

where T_1 and T_2 are the transmittances of the front and rear Sagnac loops respectively. According to Eq. (1) and (2), the final transmittance of the cascaded Sagnac filter is:

$$T_{cascaded} = \sin^2\theta_1\cos^2\left(\frac{\pi L_1\Delta n}{\lambda}\right)\sin^2\theta_2\cos^2\left(\frac{\pi L_2\Delta n}{\lambda}\right) \tag{3}$$

It can be seen from Eq. (3) that the transmission characteristics are determined by the deflection angles of the two PCs, the lengths of two PMFs, and the birefringence coefficient. The FSR of cascaded Sagnac loop filter is determined by the shorter length of PMF because the transmittance of cascaded filter is multiplied by two individual Sagnac loop filters. In our experiments, the birefringence coefficients of PMFs are all 6.79×10^{-4}, the influence of other two parameters on transmission spectrum were simulated using MATLAB. Fig. 2 shows the simulated transmission spectra of the cascaded Sagnac filter, when the length of PMFs are 3 m and 1.7 m, respectively.

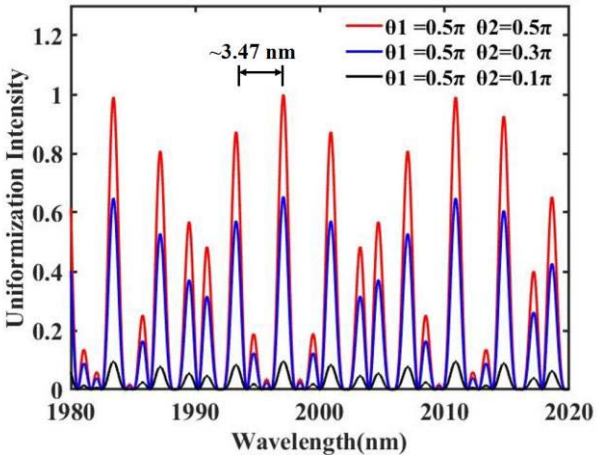

FIGURE 2. Simulated transmission spectrum of the cascaded Sagnac filter when L_1 = 3m, L_2 = 1.7m.

It can be seen from Fig.2 that the extinction ratio of filter transmission spectrum is always increases with increasing θ_1 and θ_2. This is due to the properties of the Eq. (3), when the θ_1 and θ_2 are both 0.5π, the extinction ratio reaches the maximum value. In practice, the deflection angle of the two

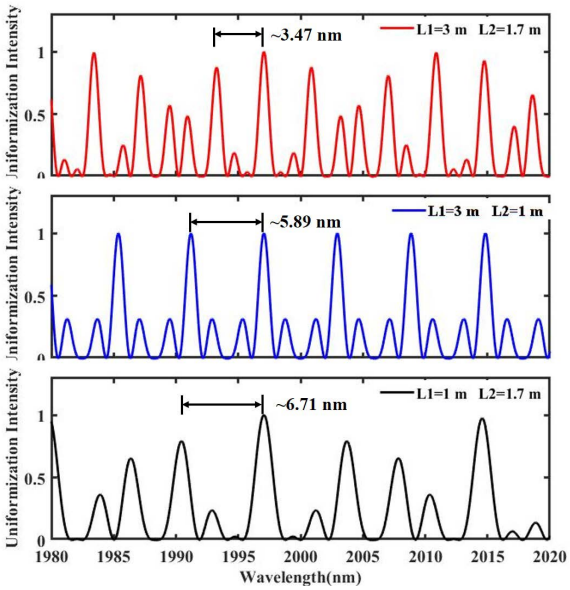

FIGURE 3. Simulated transmission spectrum of the cascaded Sagnac filter when $\theta_1 = 0.5\pi$, $\theta_2 = 0.5\pi$.

PCs is continually changed to optimize the transmission of the filters.

When θ_1 and θ_2 are fixed, the FSR of transmission spectrum varies with the length of PMFs. As shown from Fig. 3, setting the length combinations of PMF as 3/1.7, 3/1 and 1.7/1 m, respectively. The maximum extinction ratios are not varied with the length of PMFs. The FSR of simulated transmission spectra is determined by the shorter PMF according the properties of cosine function in Eq. (3).

The cascaded Sagnac loop filter is characterized by a super-continuous laser (Koheras Co., super K) and an optical spectrum analyzer (OSA), as shown in Fig.4. We set the lengths of the PMFs to be 3 m and 1.7 m. The birefringence coefficient is 6.79×10^{-4}. The transmission spectrum has the largest extinction ratio when θ_1 and θ_2 are both 0.5π. The position of the reflection peak is fixed and the extinction

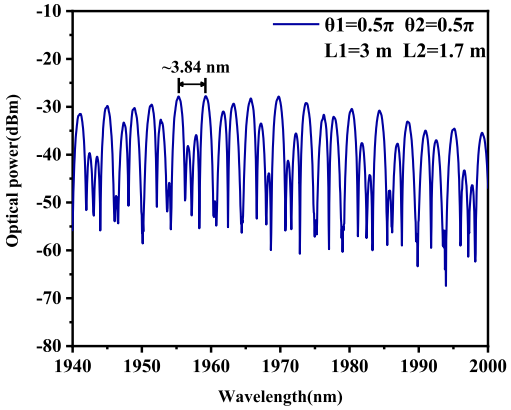

FIGURE 4. The measurement schematic of a cascaded Sagnac loop filter.

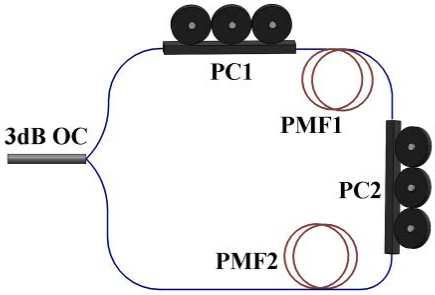

FIGURE 5. The structure of a two-segment Sagnac filter.

ratio varies with θ_1 and θ_2. The uneven spectral envelope observed in Fig. 4 arises mainly from the effect of different length of PMF1 and PMF2, and may lead to an uneven multi-wavelength lasing output in the proposed TDFL.

B. TWO-SEGMENT SAGNAC LOOP FILTER

The two-segment Sagnac filter has been the subject of considerable research because of its tunable and stable output. Its structure is shown in Fig. 2. The transmission function T of the comb filter derived from Jones matrixes is [26]:

$$T = \sin\theta_1 \sin\theta_2 \cos^2\left(\frac{2\pi L_{eff}\Delta n}{\lambda}\right) L_{eff} = \begin{cases} L_1 + L_2 \\ L_1 - L_2 \end{cases} \quad (4)$$

θ_1 and θ_2 represent the rotation angle of PC1 and PC2 respectively. L_{eff} is the effective length of PMF in the two-segment Sagnac filter. Δn is the birefringence coefficient of PMF and λ is the central wavelength of the incident light. The FSR of the two-segment Sagnac filter can be expressed as:

$$\Delta\lambda = \frac{\lambda^2}{\Delta n L_{eff}} \quad (5)$$

As shown in Fig. 6, the transmission spectrum of two-segment Sagnac filter was simulated according to the Eq. (4).

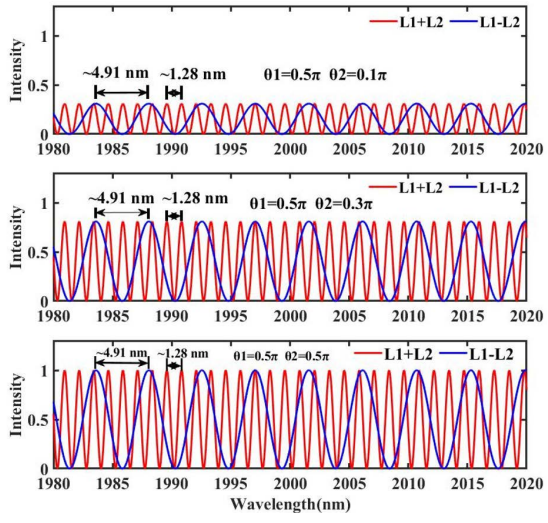

FIGURE 6. Simulated transmission spectra of the two-segment Sagnac filter when $L_1 = 3$m, $L_2 = 1.7$m.

In calculation, L_1 and L_2 are 3 m and 1.7 m, θ_1 was fixed as 0.5π, the value of θ_2 are 0.1π, 0.3π and 0.5π, respectively. The blue solid line represents the transmission spectrum of the filter when the effective length of PMF is $L_1 - L_2$, with the FSR is about 4.91 nm. The red solid line represents the transmission spectrum of the filter when the effective length of PMF is $L_1 + L_2$, with the FSR is about 1.28 nm. The extinction ratio of transmission spectrum increases with the increase of θ_2, this characteristic conforms the property of the sin function in Eq. (4). In addition, the FSRs of transmission spectrum are 4.91 nm and 1.28 nm, in good agreement with the Eq. (5).

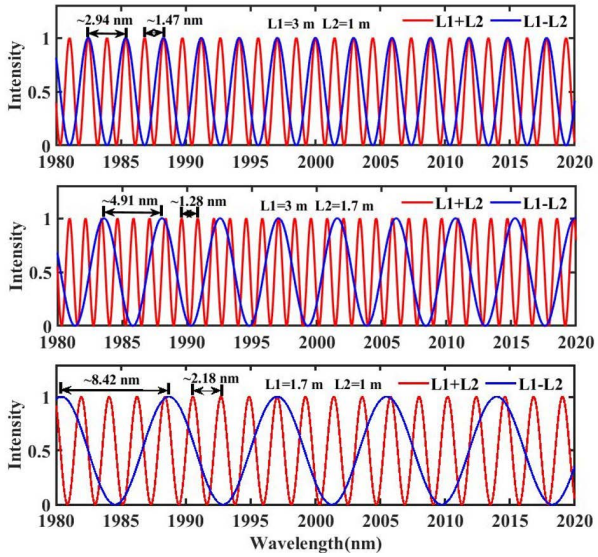

FIGURE 7. Simulated transmission spectra of the two-segment Sagnac filter when $\theta_1 = 0.5\pi$, $\theta_2 = 0.5\pi$.

Fig. 7 shows the relationship between the length of PMF and the transmission spectrum of two-segment Sagnac filter. In calculation, θ_1 and θ_2 are both 0.5π, L_1 and L_2 are 3 m/1 m, 3 m/1.7 m and 1 m/1.7 m, respectively. The FSR of transmission spectrum changes with the effective length of PMF, which is consistent with Eq. (5). When the length of PMF1 and PMF2 are 3 m and 1.7 m, the calculated FSRs are 4.91 nm and 1.28 nm.

Fig. 8 shows the experimentally measured transmission spectrum of the two-segment Sagnac loop filter. In the measurement, a super-continuous laser (Koheras Co., super K) was used as a white light source. The length of the PMFs are 3 m and 1.7 m. The birefringence coefficient is 6.79×10^{-4}. By adjusting the PCs carefully, when θ_1 and θ_2 are both 0.5π, the extinction ratio of transmission spectrum reaches maximum value and the FSRs of the two-segment Sagnac loop filter are 1.23 nm and 4.87 nm. The experimental result is in good agreement with numerical results.

III. EXPERIMENTAL SETUP AND RESULTS

Fig. 9 shows the structure of the fiber laser based on a cascaded Sagnac loop filter. The experimental system is

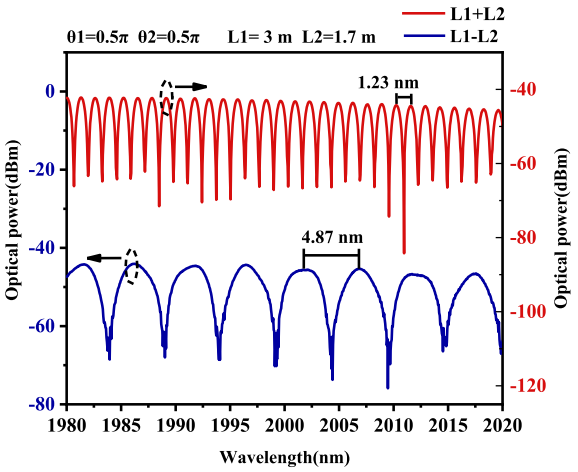

FIGURE 8. The measurement schematic of a two-segment Sagnac loop filter.

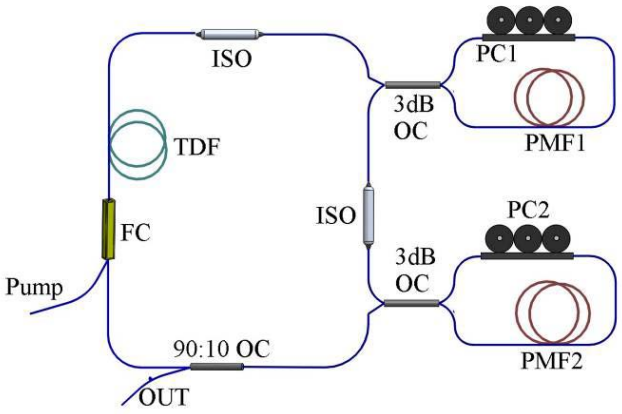

FIGURE 9. The structure of the interval-adjustable multi-wavelength TDFL-based cascaded Sagnac-loop filters.

composed of one 793-nm pump laser, one 793/2000 nm pump combiner, one 2.7-m length double-clad thulium-doped fiber (TDF), two isolators (ISOs), two 3-dB optical couplers (OCs), two polarization controllers (PCs), two polarization-maintaining fibers (PMFs), and one 90:10 coupler. The 793-nm pump light is coupled into the laser cavity by the 793/2000 nm pump combiner. The core diameter and inter-cladding diameter of the TDF are 10 μm and 130 μm, respectively, and its adsorption at 793 nm is 1.4 dB m^{-1}. To ensure unidirectional transmission, an ISO is spliced after the TDF. The cascaded Sagnac loops filter was inserted into the laser cavity with 3 m and 1.7 m PMF. The output light from the 10% port of the OC is monitored by an OSA (YOKOGAWA AQ6375) with a resolution of 0.05 nm.

In our experiment, when pump power was 2.71 W, a single-wavelength laser could be obtained by adjusting PC1 and PC2. As shown in Fig. 10, the central wavelength of the laser output is 1992.57 nm and the OSNR is about 55 dB.

To verify the stability of the single-wavelength operation, the lasing wavelength of 1992.57 nm was tested for 60 min

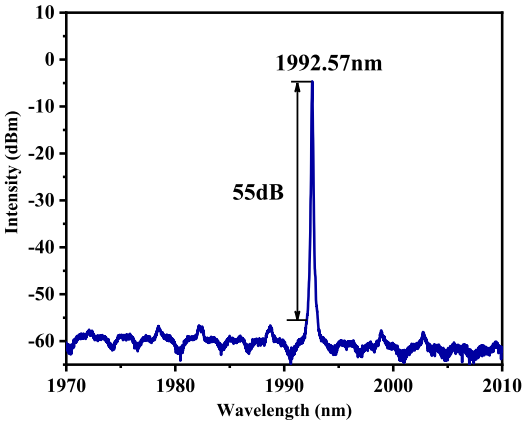

FIGURE 10. The output spectrum of a single-wavelength laser.

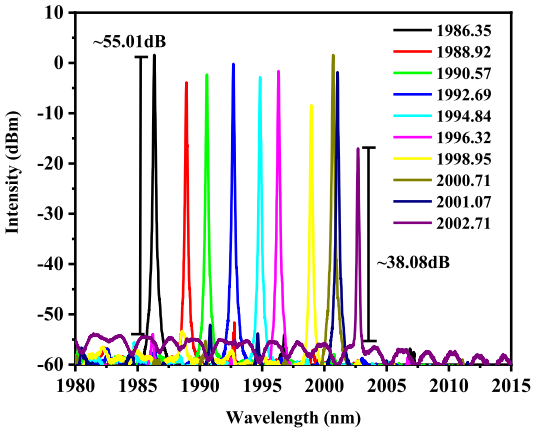

FIGURE 12. The output spectrum of switchable single-wavelength lasing.

at room temperature with no adjustment to any part of the fiber laser during this time. The stability of single-wavelength operation is shown in Fig. 11. The wavelength drift was less than ±0.02 nm and power fluctuation was less than ±0.92 dB. This indicates that our TDFL can operate stably in single-wavelength lasing.

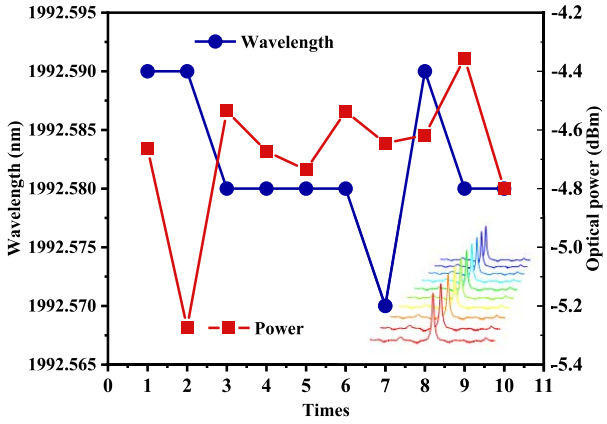

FIGURE 11. Measured output wavelength drifts and power fluctuations for ten OSA scans with a time interval of six minutes.

As shown in Fig. 12, a switchable single-wavelength lasing output can be achieved by adjusting PC1 and PC2. The switchable range was 16.36 nm, and we achieved switchable operation at 1986.35, 1988.93, 1990.57, 1992.70, 1994.84, 1996.32, 1998.95, 2000.71, 2001.06, and 2002.71 nm. The maximum and minimum of OSNR were 55.01 dB and 38.08 dB. During the adjustment of PC1 and PC2, the size of the FSR varied with the deflection angle of two PCs. Therefore, the selection interval of output wavelengths is not a fixed value.

When the pump power was 2.98 W, dual-wavelength lasing was obtained and switched by adjusting the PCs. As shown in Fig. 13, the two wavelengths were 1957.13 nm and 1988.78 nm, with the OSNR were both 28 dB. The interval of two wavelengths was 31.65 nm which is 8 times larger than the FSR of the cascaded Sagnac filter. In order to verify the fluctuation of output power and the drift of wavelength, the laser was tested for one hour and recorded every six minutes, without changing the operating parameters and operating environment. The waterfall plot on the right of Fig. 13 shows the operation state of dual-wavelength laser within one-hour.

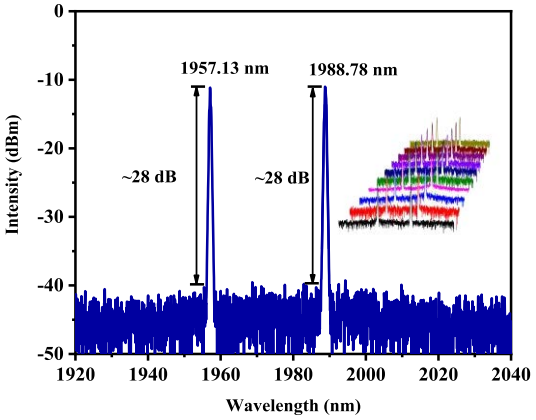

FIGURE 13. The output spectrum of a dual-wavelength laser.

According to Fig. 14, the red square and blue circle represent two output wavelengths, respectively. In the one-hour duration of the experiment, the wavelength drift of wavelength 1 was less than ±0.05 nm and the power fluctuation was less than ±0.22 dB. The wavelength drift of wavelength 2 was less than ±0.34 nm and the power fluctuation was less than ±0.94 dB. The maximum and minimum output power differences of the two lasing lines were 0.32 dB and 0.02 dB, respectively. These results verify that the TDFL is stable in dual-wavelength operation.

When the pump power was fixed at 3.34 W, different wavelength spacings were obtained for dual-wavelength operation by the appropriate rotation of PC1 and PC2. Fig. 15 and Table 1 show the outputs characteristics, the five wavelength spacings were 15.43 (lasing at 1972.28 and 1956.85 nm), 5.64 (lasing at 1973.51 and 1967.87 nm),

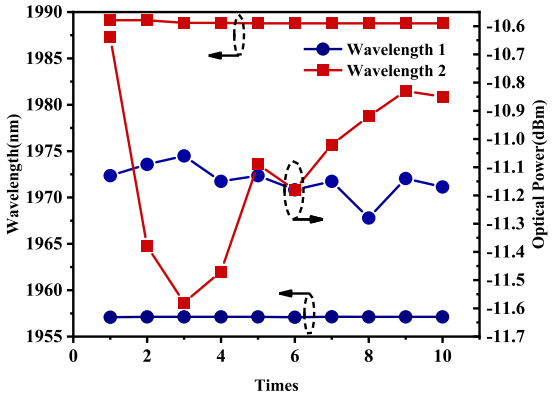

FIGURE 14. Measurements of the output wavelength drifts and the power fluctuations for ten OSA scans with a time interval of six minutes.

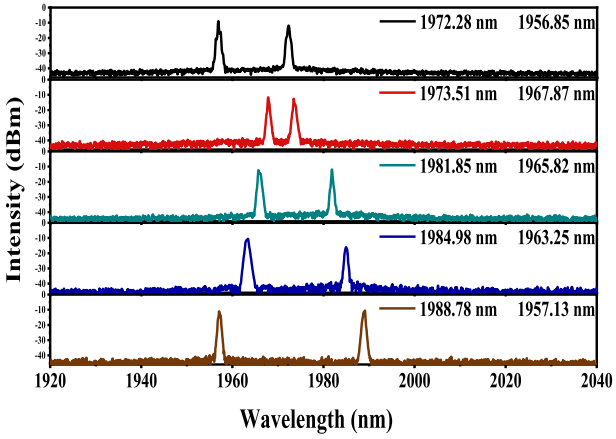

FIGURE 15. The output spectrum of a dual-wavelength laser.

TABLE 1. Switchable dual-wavelength operation condition.

Number	Wavelength interval nm	Power difference dB
1	15.43 nm	3.03 dB
2	5.64 nm	0.87 dB
3	16.03 nm	0.37 dB
4	21.73 nm	5.43 dB
5	31.65 nm	0.49 dB

16.03 (lasing at 1981.85 and 1965.82 nm), 21.73 (lasing at 1984.98 and 1963.25 nm), and 31.65 nm (lasing at 1988.78 and 1957.13 nm), and OSNR of ∼27 dB were obtained for all five dual-wavelength operations. The maximum and minimum output power differences of the two lasing wavelengths among these five cases were 5.43 dB and 0.37 dB, respectively. The stable dual-wavelength operations with different intervals were obtained depending on the extent of mode competition suppressing of the gain-equalizer aforementioned, on one hand, and the uneven spectral envelope of cascaded Sagnac filter observed in Fig. 4, on the other hand.

Moreover, when the pump power was 3.78 W, triple-wavelength outputs could be obtained, as shown in Fig. 16. The three wavelengths were 1989.69, 2000.15, and 2010.42 nm. The maximum and minimum OSNR were 57 dB and 50 dB, respectively. This is mainly because of the uneven transmission-spectrum envelope of the cascaded Sagnac loop filter. The interval between three wavelengths were 10.46 nm and 10.27 nm, any pair of wavelengths was an integral multiple of the FSR of the filter. The small figure on the right of Fig. 16 shows the measured stability of the output wavelengths at room temperature, with the test interval is 6 min, Fig. 17 is the wavelength drift and power fluctuation of triple-wavelength lasing.

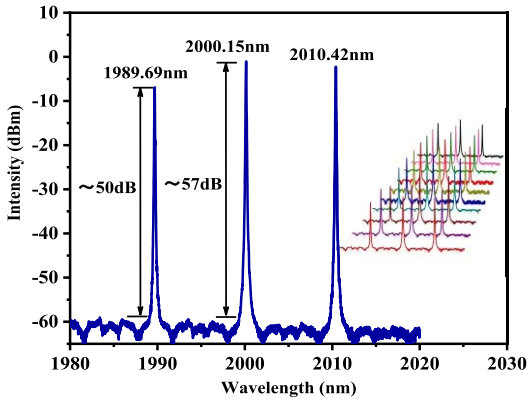

FIGURE 16. The output spectrum of a triple-wavelength laser.

The maximum and minimum power fluctuations of three wavelengths were 11.67 dB and 0.24 dB and the wavelength drift was less than ±0.1 nm. This phenomenon was caused by intense mode competition in the laser cavity. The intensity-dependent loss caused by two cascaded Sagnac loop filters is not enough to completely overcome the intense mode competition. This measurement result demonstrated that our TDFL can operate with triple-wavelength output.

With further adjustment of the PCs and increase of the pump power to 4.01 W, quadruple-wavelength lasing can be achieved. From the Fig18, the central wavelengths of four wavelengths were 1961.17, 1966.70, 1976.65 and 1982.46 nm, with the wavelength intervals were 5.53, 9.95 and 5.81 nm. The minimum and maximum OSNRs were 23 dB and 28 dB, respectively. Because of the action of intense mode competition in the laser cavity and the external environmental disturbance, the quadruple-wavelength operation did not show satisfactory stability.

To demonstrate the stability of quadruple-wavelength operation, the output spectra were measured at room temperature over 60 min, with the measured spectra shown in Fig. 18. As shown in Fig. 19, the wavelength drifts of four wavelengths were less than ±0.53, ±0.04, ±0.05 and ±0.05 nm, respectively. The output power fluctuations of four wavelengths were less than ±0.60, ±1.23, ±0.38 and ±0.06 dB, respectively. These results verify that the TDFL is also stable in quadruple-wavelength operation.

Furthermore, When the pump power was 4.6 W, quintuple-wavelength lasing was also achieved in Fig. 20. The five

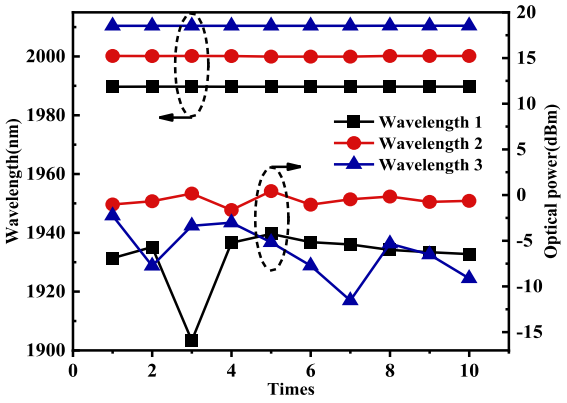

FIGURE 17. Measurements of the output wavelength drifts and the power fluctuations for ten OSA scans with a time interval of six minutes.

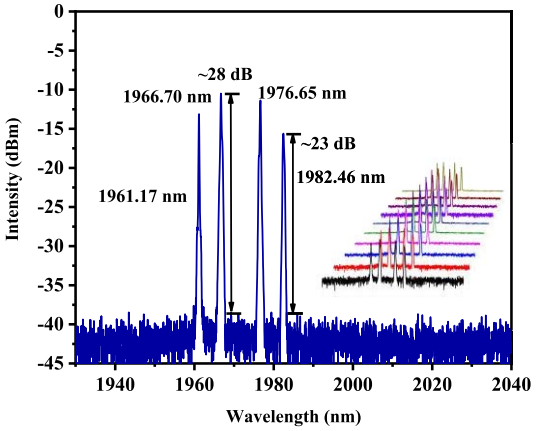

FIGURE 18. The output spectrum of a quadruple-wavelength laser.

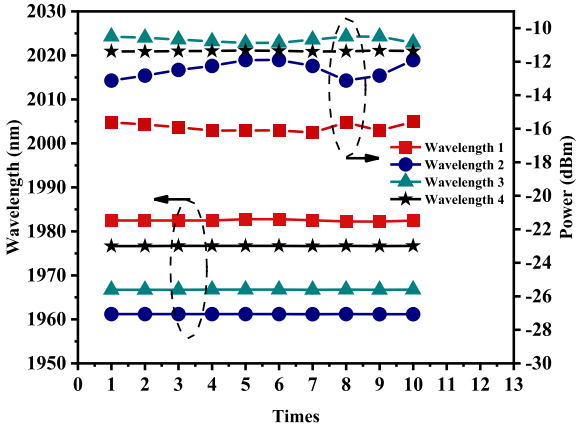

FIGURE 19. The output spectrum of a quadruple-wavelength laser.

wavelengths were 1997.55, 2001.02, 2005.01, 2007.99 and 2011.96 nm. As shown in Fig. 20, the minimum and maximum OSNRs were 28 dB and 35 dB, respectively. Because of the action of intense mode competition in the laser cavity, the quintuple-wavelength operation did not show satisfactory stability. Therefore, other stabilizing mechanisms should be introduced into the laser cavity to inhibit mode competition

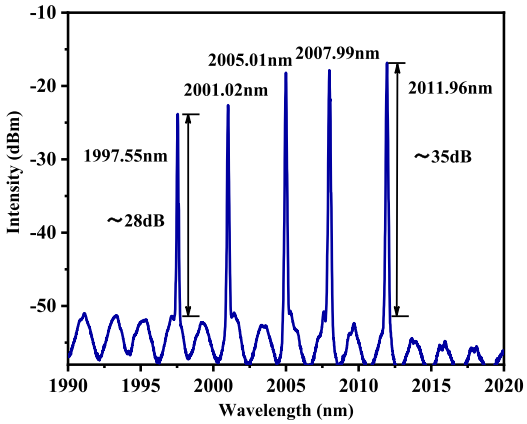

FIGURE 20. The output spectrum of quintuple-wavelength lasing.

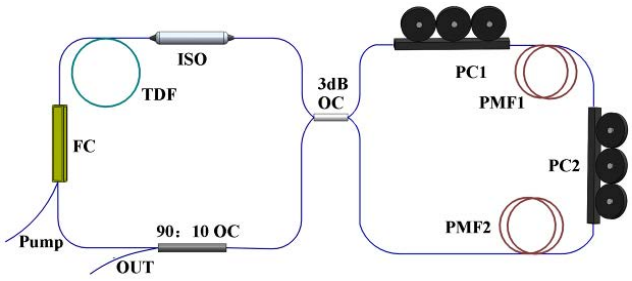

FIGURE 21. The structure of the interval-adjustable multi-wavelength TDFL-based on two-segment Sagnac loop filter.

and obtain stable multi-wavelength lasing. Unfortunately, this will lead to greater complexity of the laser system, which may be unfavorable for high-output performance in single- or dual-wavelength operation.

The work reported in Section 2 shows that a cascaded Sagnac loop filter and a two-segment Sagnac loop filter are similar in structure and principle. We used the same amplification-of-spontaneous-emission (ASE) source in the following experiment. The cascaded Sagnac loop filter is replaced by a two-segment Sagnac loop filter in order to compare the influences on the output wavelengths. Fig. 12 shows the experimental structure of the multi-wavelength Tm^{3+}-doped fiber laser incorporating a two-segment Sagnac loop filter. The same 793-nm pump source and 2.7-m long thulium-doped gain fiber are used in this fiber laser. An ISO is connected after the ASE source to ensure one-way transmission of light in the loop. The two-segment Sagnac loop filter is coupled into the laser loop with a 3-dB OC. Ten percent of the light is output by a 90:10 OC and monitored by an OSA (YOKOGAWA AQ6375) with a resolution of 0.05 nm. In this two-segment Sagnac loop filter, PMF1 is sandwiched between PC1 and PC2, and PMF2 is connected after PC2. To achieve better comparison with the cascaded Sagnac loop filter, the lengths of PMF1 and PMF2 are taken to be 3 m and 1.7 m, respectively.

In the experiment, when the pump power was fixed at 2.13 W and the two PCs were fixed in an appropriate angle,

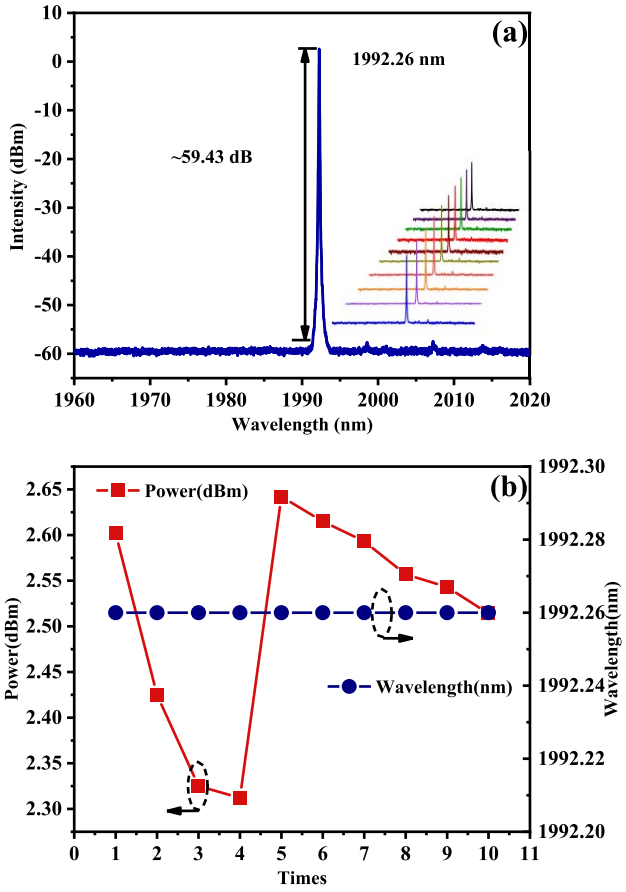

FIGURE 22. (a) The output spectrum of a single-wavelength laser. (b) Measured output wavelength drifts and power fluctuations for ten OSA scans at intervals of six minutes.

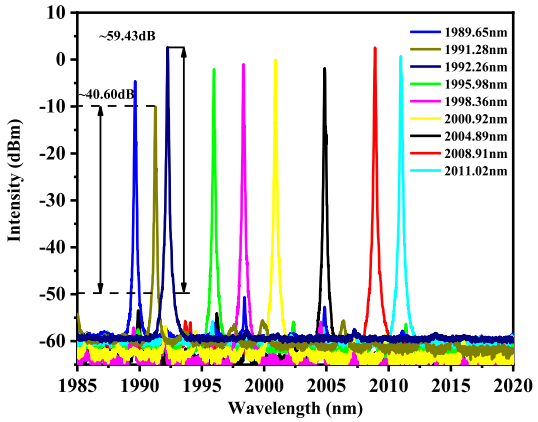

FIGURE 23. The output spectrum of switchable single-wavelength lasing.

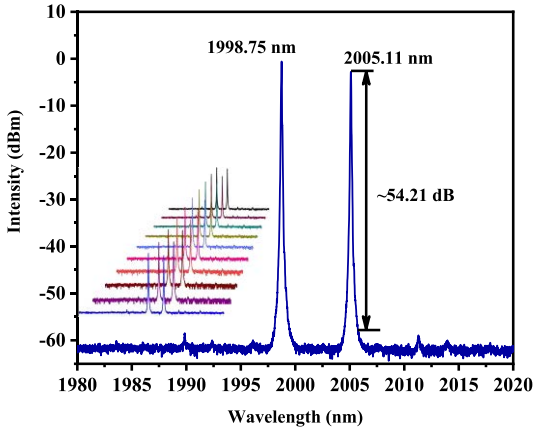

FIGURE 24. The output spectrum of a dual-wavelength laser.

a single wavelength could be lased, as shown in Fig. 22(a). The central wavelength was 1992.26 nm and the OSNR was about 59.43 dB. In order to test the wavelength and power stability of the proposed single-wavelength mode at 1992.26 nm, the wavelength data are recorded every six minutes at room temperature for one hour.

Fig. 22(b) shows the wavelength drift and power fluctuation of single-wavelength. During the testing, the power fluctuation of the measured single-wavelength mode was less than ±0.35 dB and the wavelength was stable without drift. This indicates that our TDFL can operate stably in single-wavelength lasing. From Figs. 11 and Fig. 22, one sees that when the output is operating in single-wavelength mode, the TDFL with a two-segment Sagnac loop filter has better stability.

Through adjusting PC1 and PC2 carefully, we achieved single-wavelength selectable frequencies at 1989.65, 1991.28, 1992.26, 1995.98, 1998.36, 2000.92, 2004.89, 2008.91, and 2011.02 nm with a pump power of 2.13 W, Fig.23 documents the tunable result. The width of switchable wavelengths was 21.37 nm. The maximum and minimum of OSNR were 59.43 dB and 40.60 dB. The FSR of the two-segment Sagnac loop filter changed with the variation of PC's deflection angle. There is no obvious multiple relationship between switchable wavelength interval and the filter FSR.

Through careful adjustment of PC1 and PC2, the dual-wavelength operation was obtained with 3.12 W pump power. As shown in Fig. 24, the two wavelengths were 1998.75 and 2005.11 nm. The interval between them, 6.36 nm, was proportional to the FSR of the filter. The OSNR for two wavelengths were both greater than 54.21 dB. Operating the dual-wavelength laser for one hour and recording its power fluctuation and wavelength drift every six minutes, the test results were showed in Fig. 24, bottom left, and recorded in Fig. 25. The power fluctuation at each wavelength was less than ±3 dB and the wavelength drift was less than ±0.1 nm. This indicates that the laser can operate stably in the dual-wavelength mode.

Achieving switchable dual-wavelength operation depends on the proposed fiber laser-based two-segment Sagnac loop filter, as shown in Fig. 26. The operating conditions for the switchable dual-wavelength laser are recorded in Table 2.

There are five switchable dual-wavelength modes: 1989.99/1998.79 nm, 1996.63/2012.30 nm, 1991.10/2005.80 nm, 1998.70/2005.30 nm, and 1996.60/1990.01 nm. The wavelength intervals were 8.8, 15.67, 14.7, 6.6, and

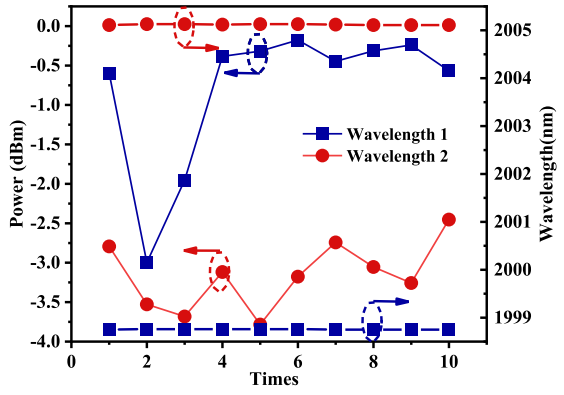

FIGURE 25. Measured output wavelength drifts and power fluctuations for ten OSA scans at intervals of six minutes.

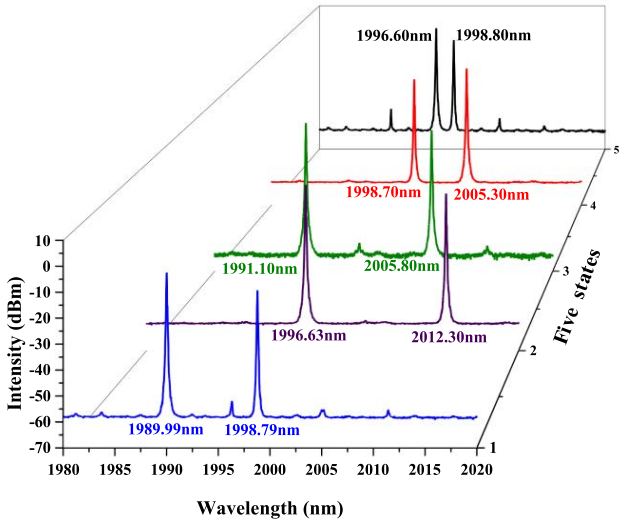

FIGURE 26. The output spectrum of the switchable dual-wavelength laser.

TABLE 2. Switchable dual-wavelength operation condition.

Number	Wavelength interval nm	Power difference dBm
1	8.80 nm	6.82 dB
2	15.67 nm	3.77 dB
3	14.70 nm	3.40 dB
4	6.60 nm	5.59 dB
5	2.20 nm	6.66 dB

2.2 nm, respectively. The outputs larger than 48 dB were obtained for all five dual-wavelengths operations. The maximum and minimum output power differences of the two lasing wavelengths among these five cases were 6.82 dB and 3.40 dB. This disequilibrium between wavelengths at dual-wavelength output was caused by the uneven transmission spectrum envelope of the two-segment Sagnac loop filter.

Fig. 27 is the output spectrum of triple-wavelength operation with the suitable polarization angle and 3.72 W pump power. The three wavelengths were 1956.85, 1972.17 and 1988.49 nm, respectively. The intervals of three wavelengths were 15.32 nm and 16.32 nm, which were approximate multiples of FSR in Fig. 8. The maximum output optical power

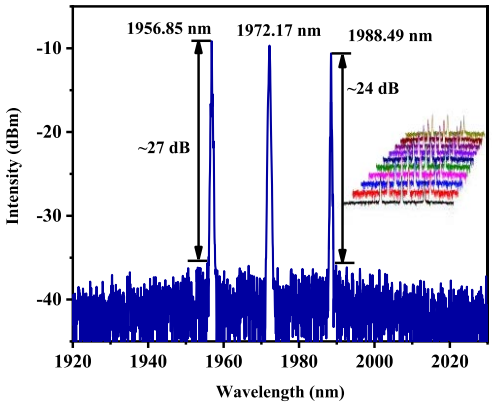

FIGURE 27. The output spectrum of a triple-wavelength laser.

was about 27 dBm in 1956.85 nm and the minimum value was 24 dB in 1988.48 nm. In order to verify the stability of triple-wavelength operation, ten experimental results were recorded at six-minute intervals without changing the external environment and experimental equipment. The waterfall plot of optical spectrum is shown in the right side of Fig. 27.

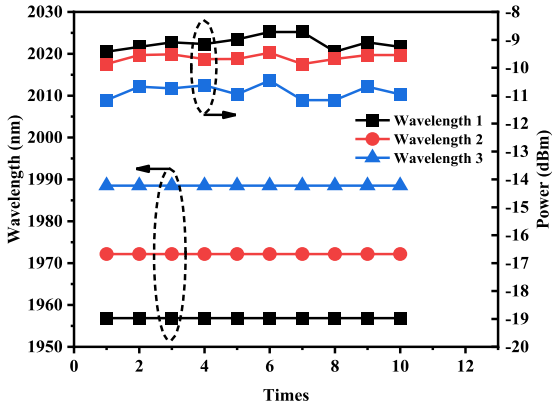

FIGURE 28. Measured output wavelength drifts and power fluctuations for ten OSA scans at intervals of six minutes.

According to the Fig. 28, the wavelength drifts of three wavelengths were less than ±0.01, ±0.02 and ±0.01 nm, respectively. The power fluctuations of three wavelengths were less than ±0.71, ±0.40 and ±0.71 dB, respectively. The output results of TDFL with two-segment Sagnac filter are better than cascaded Sagnac filter in both wavelength drifts and power fluctuations.

As shown in Fig. 29, to facilitate comparison with the laser in Section 1, the quadruple wavelengths can be output with careful adjustment PCs simultaneously. The pump power was 4.33 W, and the four wavelengths were 1994.43, 2000.71, 2009.59, and 2016,06 nm. The OSNR of the output wavelengths was greater than 53.49 dB. The three wavelength intervals were 6.28, 8.88, and 6.47 nm, these intervals being approximate multiples of the 1.23-nm FSR of the two-segment Sagnac filter. The stability of the output wavelength when using a two-segment Sagnac loop filter was also measured, with the results being monitored every six minutes without changing the laboratory environment or other

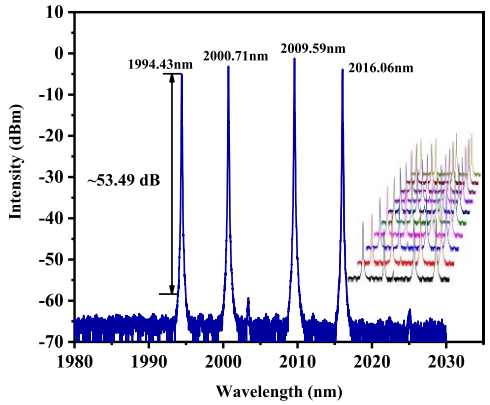

FIGURE 29. The output spectrum of a quadruple-wavelength laser.

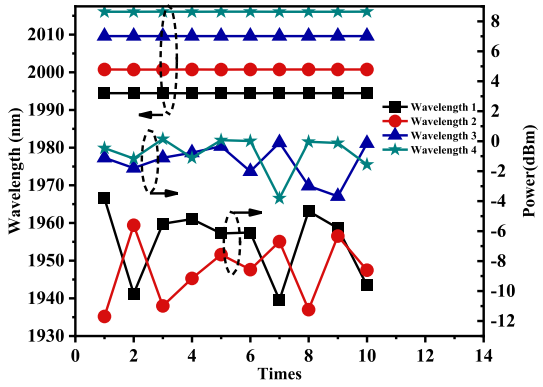

FIGURE 30. Measurement of the output wavelength drifts and power fluctuations for ten OSA scans at six-minute intervals.

experiment parameters. Fig. 30 shows that the quadruple-wavelength wavelength drifts were both less than ±0.5 nm and that the power fluctuations were less than ±7 dB. The main reason for wavelength drift and power fluctuation was the mode competition in laser cavity in the constant-temperature laboratory environment.

It can be seen that the number of wavelengths obtained with cascaded Sagnac loop filter is more than with a two-segment Sagnac loop filter, but the stability and OSNR are slightly worse than those of the two-segment Sagnac loop filter. Because of its more flexible FSR range, a two-segment Sagnac loop filter can be utilized to realize wavelength selection and interval tuning operation of dual-wavelength output. When the output has the same number of wavelengths, the laser that uses two-segment Sagnac loop filter always has a lower laser threshold. This is because the second fiber laser has a simpler structure.

IV. CONCLUSION

In summary: A switchable multi-wavelength thulium-doped fiber laser, with the assistance of a cascaded Sagnac loop filter or two-segment Sagnac loop filter, is proposed and demonstrated. The structure and principles of the cascaded Sagnac loop filter and the two-segment Sagnac loop filter are analyzed and compared. The wavelength can be switched by adjusting the polarization states of PC1 and PC2. When the cascaded Sagnac loop is utilized as the comb filter, the laser output can reach up to five wavelengths with a maximum OSNR of 35 dB. With adjustment of the PCs, there are ten wavelengths that can be switched, from 1986.35 to 2002.71 nm. When a two-segment Sagnac loop is used to replace the cascaded Sagnac loop, the flexibility of switchable output wavelengths is increased although the number of output wavelengths is slightly reduced. The stability of the output wavelengths is also improved with the use of a two-segment Sagnac loop filter. This is mainly because of the characteristics of the two-segment Sagnac loop filter. In addition, the variation of external environment will influence the output performance of lasers, such as temperature, vibration and so on, this is a very important point and will be left for future consideration. Both of the proposed multi-wavelength thulium-doped fiber lasers (TDFLs) are simple in structure and flexible in operation, and can be utilized in many fields that require switchable output, such as optical communication and military detection.

REFERENCES

[1] M. Tao, B. Tao, Z. Hu, G. Feng, X. Ye, and J. Zhao, "Development of a 2 μm Tm-doped fiber laser for hyperspectral absorption spectroscopy applications," *Opt. Exp.*, vol. 25, no. 26, pp. 32386–32394, Dec. 2017.

[2] D. Ouyang, J. Zhao, Z. Zheng, M. Liu, S. Ruan, and J. Pei, "Repetition-rate-switchable and self-mode-locked pulses generation from a gain-switched thulium-doped fiber laser and their amplification properties," *IEEE Photon. J.*, vol. 9, no. 4, Aug. 2017, Art. no. 1503710.

[3] L. Zhang, J. Zhang, Q. Sheng, C. Shi, W. Shi, and J. Yao, "Watt-level 1.7-μm single-frequency thulium-doped fiber oscillator," *Opt. Exp.*, vol. 29, no. 17, pp. 27048–27056, Aug. 2021.

[4] H. Huang, S. Wang, H. Chen, O. L. Antipov, S. S. Balabanov, and D. Shen, "High power simultaneous dual-wavelength CW and passively-*Q*-switched laser operation of LD pumped Tm:YLF at 1.9 and 2.3 μm," *Opt. Exp.*, vol. 27, no. 26, pp. 38593–38601, Dec. 2019.

[5] A. A. Kolegov, A. V. Chernikova, A. O. Leshkov, and E. A. Belov, "Thulium fiber laser with wavelength 1908 nm," *J. Opt. Technol.*, vol. 84, no. 8, pp. 30–34, Aug. 2017.

[6] S. Liu, F. Yan, Y. Li, L. Zhang, Z. Bai, H. Zhou, and Y. Hou, "Noise-like pulse generation from a thulium-doped fiber laser using nonlinear polarization rotation with different net anomalous dispersion," *Photon. Res.*, vol. 4, no. 6, pp. 318–321, Dec. 2016.

[7] K. Jiang, Z. Wu, S. Fu, J. Song, H. Li, M. Tang, P. Shum, and D. Liu, "Switchable dual-wavelength mode-locking of thulium-doped fiber laser based on SWNTs," *IEEE Photon. Technol. Lett.*, vol. 28, no. 19, pp. 2019–2022, Oct. 1, 2016.

[8] J. Liu, C. Liu, H. Shi, and P. Wang, "High-power linearly-polarized picosecond thulium-doped all-fiber master-oscillator power-amplifier," *Opt. Exp.*, vol. 24, no. 13, pp. 15005–15011, Jun. 2016.

[9] X. Ma, D. Chen, Q. Shi, G. Feng, and J. Yang, "Widely tunable thulium-doped fiber laser based on multimode interference with a large no-core fiber," *J. Lightw. Technol.*, vol. 32, no. 19, pp. 3234–3238, Oct. 1, 2014.

[10] S. Zhang, T. Geng, H. Niu, X. Li, Y. Yan, C. Sun, S. Deng, Z. Wang, S. Wang, W. Yang, W. Sun, and L. Yuan, "All fiber compact bending sensor with high sensitivity based on a multimode fiber embedded chirped long-period grating," *Opt. Lett.*, vol. 45, pp. 4172–4175, Aug. 2020.

[11] W. Liu, Y. Zu, Y. Wang, Z. Zhang, J. Liu, and L. Su, "Active *Q*-switching operation of a Tm:SrF_2 single crystal fiber laser near 2 μm," *Opt. Mater. Exp.*, vol. 11, no. 9, pp. 2877–2882, Sep. 2021.

[12] L. Zhang, F. Yan, T. Feng, Y. Guo, Q. Qin, H. Zhou, and Y. Suo, "Switchable multi-wavelength thulium-doped fiber laser employing a polarization-maintaining sampled fiber Bragg grating," *IEEE Access*, vol. 7, pp. 155437–155445, 2019.

[13] T. Kasamatsu, Y. Yano, and T. Ono, "1.49-μm-band gain-shifted thulium-doped fiber amplifier for WDM transmission systems," *J. Lightw. Technol.*, vol. 20, no. 10, pp. 1826–1838, Oct. 2002.

[14] R. Mizushima, T. Detani, C. Zhu, P. Wang, H. Zhao, and H. Li, "The superimposed multi-channel helical long-period fiber grating and its application to multi-channel OAM mode generator," *J. Lightw. Technol.*, vol. 39, no. 10, pp. 3269–3275, May 15, 2021.

[15] S. Liu, F. Yan, W. Peng, T. Feng, Z. Dong, and G. Chang, "Tunable dual-wavelength thulium-doped fiber laser by employing a HB-FBG," *IEEE Photon. Technol. Lett.*, vol. 26, no. 18, pp. 1809–1812, Sep. 15, 2014.
[16] H. Wei, Z. Lianqing, D. Mingli, and L. Fei, "A 1.8-μm multiwavelength thulium-doped fiber laser based on a hybrid interference filter," *Int. J. Optomechatron.*, vol. 10, nos. 3–4, pp. 154–161, Oct. 2016, doi: 10.1080/15599612.2016.1230914.
[17] J. Li, X. Chen, M. Lv, Y. Gao, and G. Chen, "16-port tunable fiber laser based on a digital micromirror device in C-band," *Appl. Phys. B, Lasers Opt.*, vol. 125, no. 2, Jan. 2019, Art. no. 30.
[18] M. Wang, Y. Huang, L. Yu, Z. Song, D. Liang, and S. Ruan, "Multiwavelength thulium-doped fiber laser using a micro fiber-optic Fabry–Pérot interferometer," *IEEE Photon. J.*, vol. 10, no. 4, pp. 1–8, Aug. 2018.
[19] T. Feng, M. Jiang, Y. Ren, M. Wang, F. Yan, Y. Suo, and X. S. Yao, "High stability multiwavelength random erbium-doped fiber laser with a reflecting-filter of six-superimposed fiber-Bragg-gratings," *OSA Continuum*, vol. 2, pp. 2526–2538, Sep. 2019.
[20] W. Jin, Y. Qi, Y. Yang, Y. Jiang, Y. Wu, Y. Xu, S. Yao, and S. Jian, "Switchable dual-mode all-fiber laser with few-mode fiber Bragg grating," *J. Opt.*, vol. 19, no. 9, Sep. 2017, Art. no. 095702.
[21] Y. Guo, F. Yan, T. Feng, Q. Qin, Z. Bai, T. Li, W. Han, H. Zhou, and Y. Suo, "Wavelength-interval-switchable multi-wavelength thulium-doped fiber laser with a nonlinear dual-pass Mach–Zehnder interferometer filter in 2-μm-band," *Opt. Laser Technol.*, vol. 145, Jan. 2022, Art. no. 107470.
[22] A. W. Al-Alimi, N. A. Cholan, M. H. Yaacob, A. F. Abas, M. T. Alresheedi, and M. A. Mahdi, "Wide bandwidth and flat multiwavelength Brillouin-erbium fiber laser," *Opt Exp.*, vol. 25, no. 16, pp. 19382–19390, Aug. 7, 2017.
[23] T. Feng, D. Wei, W. Bi, W. Sun, S. Wu, M. Jiang, F. Yan, Y. Suo, and X. S. Yao, "Wavelength-switchable ultra-narrow linewidth fiber laser enabled by a figure-8 compound-ring-cavity filter and a polarization-managed four-channel filter," *Opt. Exp.*, vol. 29, no. 20, pp. 31179–31200, Sep. 2021.
[24] Y. Li, Y. Shen, J. Tian, Q. Fu, and Y. Yao, "Wavelength switchable multi-wavelength erbium-doped fiber laser based on polarization-dependent loss modulation," *J. Lightw. Technol.*, vol. 39, no. 1, pp. 243–250, Jan. 1, 2021.
[25] Y. Zhang, J. Ye, X. Ma, J. Xu, J. Song, T. Yao, and P. Zhou, "High power tunable multiwavelength random fiber laser at 1.3 μm waveband," *Opt. Exp.*, vol. 29, no. 4, pp. 5516–5524, Feb. 2021.
[26] R. M. Sova, C.-S. Kim, and J. U. Kang, "Tunable all-fiber birefringence comb filter," in *Tech. Dig. Opt. Fiber Commun. Conf.*, Anaheim, CA, USA, 2002, pp. 698–699, Paper ThGG61.

TING LI received the M.S. degree from the School of Optical Engineering, Minzu University, in 2019. He is currently pursuing the Ph.D. degree with the Key Laboratory of All Optical Network and Advanced Telecommunication Network, Ministry of Education, Institute of Lightwave Technology (ILT), Beijing Jiaotong University. His current research interests include rare-earth doped optical laser and multi-wavelength fiber laser.

FENGPING YAN received the B.S. degree from the Hefei University of Technology, Hefei, China, in 1989, and the Ph.D. degree from Beijing Jiaotong University, Beijing, China, in 1996. In 1996, he joined the Institute of Lightwave Technology (ILT), Beijing Jiaotong University, and was promoted as an Associate Professor, in 1998. From 2001 to 2002, he was the National Senior Visiting Scholar at the Osaka Institute of Technology, Osaka, Japan. In 2003, he was a Full Professor and became the Vice Director of ILT, Beijing Jiaotong University. In 2018, he was the Director of ILT, Beijing Jiaotong University. He has published more than 240 papers, written one book, and held more than 50 patents. His research interests include rare-earth-doped fibers, fiber lasers, optical wavelength switching, all optical networks, and metamaterials research. He was chairing two projects funded by the National High Technology Research and Development Program of China (863 Program), in 1996 and 2002. He has been chairing nine projects funded by the National Natural Science Foundation of China, since 2000.

DAN CHENG is currently pursuing the Ph.D. degree in fiber laser technology with the Key Laboratory of All Optical Network and Advanced Telecommunication of Electromagnetic Compatibility, Institute of Lightwave Technology, Beijing Jiaotong University, Beijing, China.

QI QIN received the M.S. degree in communication and information system from the Key Laboratory of All Optical Network and Advanced Telecommunication Network, Ministry of Education, Institute of Lightwave Technology (ILT), Beijing Jiaotong University, in 2019, where he is currently pursuing the Ph.D. degree. His research interests include optical fiber components and optical fiber-based devices.

YING GUO received the M.S. degree from the School of Information Engineering, Zhengzhou University, in 2010. She is currently pursuing the Ph.D. degree with the Key Laboratory of All Optical Network and Advanced Telecommunication Network, Ministry of Education, Institute of Lightwave Technology (ILT), Beijing Jiaotong University. She joined the Zhongyuan University of Technology for teaching, in 2010. Her current research interests include rare-earth doped optical laser and multi-wavelength fiber laser.

TING FENG received the Ph.D. degree in communication and information system from Beijing Jiaotong University, Beijing, China, in January 2015.

From September 2012 to September 2013, he was a Visiting Scholar with the Optics Laboratory, School of Electrical and Computer Engineering, Georgia Institute of Technology, Atlanta, GA, USA. He joined the Photonics Information Innovation Center, College of Physics Science and Technology, Hebei University, Baoding, China, in 2015, where he was promoted as a Full Professor, in 2021. In 2020, he was promoted as an Outstanding Young Scholar of Hebei province and a Hebei New Century "333 Talent Project" suitable person. He has chaired and participated in more than ten research projects funded by the National Natural Science Foundation of China and Natural Science Foundation of Hebei Province. He has authored more than 90 refereed journal articles and written two optics related books. He has been granted with more than 30 patents in related areas. His research interests include optical fiber lasers, optical fiber sensing, and their application technologies. He is a member of the Optical Society of America (OSA) and a member of the Chinese Optical Society (COS).

ZHUOYA BAI is currently pursuing the Ph.D. degree in electro-optical system with the Key Laboratory of All Optical Network and Advanced Telecommunication of Electromagnetic Compatibility, Institute of Lightwave Technology, Beijing Jiaotong University, Beijing, China.

XUEMEI DU received the master's degree in electronic science and technology from Beijing Jiaotong University, in 2017, where she is currently pursuing the Ph.D. degree in information and communication engineer with the Key Laboratory of All Optical Network and Advanced Telecommunication Network, Ministry of Education, Institute of Lightwave Technology (LIT). Her current research interests include the research and application of metamaterial absorbers and the integration of two-dimensional novel materials.

YUPING SUO received the M.S. and Ph.D. degrees in obstetrics and gynecology from the Heilongjiang University of Chinese Medicine, Harbin, China, in 1999 and 2002, respectively. She finished her postdoctoral research in clinical medicine at Sichuan University, Chengdu, China, in 2005. She was with the Shanxi Provincial People's Hospital, Taiyuan, China. She was a Professor of gynecological oncology with Shanxi Medical University, Taiyuan, in 2014. She was promoted as an Outstanding Expert of Shanxi Province, in 2017. She is currently an Academic Leader of Shanxi Province and serves as the Chairman for the Gynecological Tumor Management Committee of Shanxi Province. She has published more than 50 articles and chaired or participated in more than ten scientific research projects. Her main research interests include the pathogenesis and prevention of ovarian cancers and laser photodynamic therapy of ovarian cancers. She was a recipient of one provincial first prize of scientific and technological progress.

HONG ZHOU received the B.S. degree in electronic engineering from Tsinghua University, in 1983, and the M.S. and Ph.D. degrees in electronic engineering from Kyoto University, in 1987 and 1991, respectively. He is currently a Professor with the Department of Electronic Information and Communication Engineering, Osaka Institute of Technology. His current research interests include high-speed optical communication, wireless networks, and optical wireless communication.